Available online at www.sciencedirect.com

ScienceDirect

Transportation Research Procedia 40 (2019) 405–412

Transportation Research Procedia

www.elsevier.com/locate/procedia

13th International Scientific Conference on Sustainable, Modern and Safe Transport (TRANSCOM 2019), High Tatras, Novy Smokovec – Grand Hotel Bellevue, Slovak Republic, May 29-31, 2019

Design of an electronic odometer for DC motors

Dušan Nemec[a]*, Aleš Janota[a], Marián Hruboš[a], Vojtech Šimák[a]

[a]*University of Zilina, Faculty of Electrical engineering, Department of Control and Information Systems, Univerzitna 1, 01026 Zilina, Slovakia*

Abstract

The paper proposes an innovative electronic sensor for odometry in mobile robotics. The sensor is based on measurement of current peaks caused by commutation of a DC electric motor. The signal is preprocessed by analog filters, then digital processing in microcontroller is applied. The sensor utilizes small low-power MCU AtTiny44 and provides SPI interface for the communication with the master robot controller. The main advantage of the proposed sensor is the lack of any mechanical parts, which results in high durability. The sensor has been simulated in Simulink and then a fully-functional sample was created and tested.

Peer-review under responsibility of the scientific committee of the 13th International Scientific Conference on Sustainable, Modern and Safe Transport (TRANSCOM 2019).

Keywords: odometry; sensorless odometer; DC motor; commutator

1. Introduction

Brushed DC motors with permanent magnets are widely used in many industrial, automotive or household applications. Their great advantage over modern brushless DC motors (BLDC) is the simplicity of the control driver (single H-bridge with PWM control signal is sufficient). On the other hand, BLDC motors have greater efficiency and durability (no mechanical commutator is present). While the position and speed control of BLDC motors is straightforward (BLDC is a synchronous motor), brushed DC motors require sensing of the current speed. In mobile robotics, the position of the motor's rotor is required to estimate the position of the robot.

The commonly-used approach utilizes an external permanent magnet mounted at the end of the motor's shaft. The orientation of the magnet is then sensed by Hall effect sensors (Rapos et al. (2016)). The output voltage of the Hall

* Corresponding author. Tel.: +421 41 513 3301
E-mail address: dusan.nemec@fel.uniza.sk

2352-1465
Peer-review under responsibility of the scientific committee of the 13th International Scientific Conference on Sustainable, Modern and Safe Transport (TRANSCOM 2019).
10.1016/j.trpro.2019.07.059

effect sensor contains pulses corresponding to the presence of the permanent magnet nearby the sensor. Rotating permanent magnet may cause electromagnetic interference in nearby electronics and mechanical vibrations of the shaft. It increases the overall length of the motor and requires non-metallic enclosing to prevent pollution of the magnet by ferromagnetic dust. If the shaft of the DC motor is not designed (long enough) to bear the external sensor, an additional installation of the sensor may be problematic.

The permanent magnet may be replaced with an optical encoder or slotted plate (Chotai and Narwekar (2017)). The position of the rotor is then detected by optoelectronic sensors (e.g. phototransistors). Authors Kumar and Banavar (2017) have proposed an observer to estimate the position of the motor at very low speeds in order to avoid quantization noise.

Another approach may measure the induced voltage in the rotor (back EMF) since it is proportional to the speed of the rotor (see e.g. Kamdar et al. (2015)):

$$u_{\text{bemf}} = K_u \omega \tag{1}$$

where K_u is the constant of back EMF and ω is the current angular velocity of the rotor. The simplified equivalent scheme of the brushed DC motor is in Fig. 1.

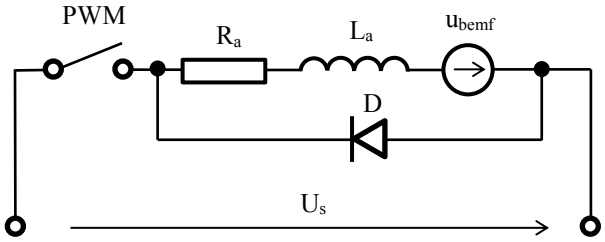

Fig. 1. Simplified equivalent scheme of a DC motor.

If we use PWM to control the motor, the flyback diode D is required to protect the switch from the voltage spikes generated by the armature (winding) inductance L_a. When the PWM switch is in "off" state, after discharge of the inductance the voltage across motor is equal to u_{bemf}. Such method allows only low PWM frequency and lower duty cycle ("off" state must be long enough for armature current to settle down).

Similar method to our method is described in Afjei et al. (2007), where authors rely on high voltage pulses caused by non-optimal commutation. These pulses may and may not occur depending on the construction of the commuter. Ramli et al. (2010) use adaptive filters to detect the primary periodic component of the DC motor's current ripple. Vazquez et al. (2016) estimated the speed of the motor from frequency analysis of its current and by correlation of the obtained spectrum with the expected spectrum. Their approach has been validated only in narrow interval of the motor speed (from 2000 to 3000 RPM).

2. Our method

We propose to detect the changes of the armature's impedance caused by non-zero size of the commutator brushes. During each period, each brush shorts one or more winding coils for a while (see Fig. 2.). This results in periodic decreasing and increasing of the armature's impedance, which causes spikes in supply current.

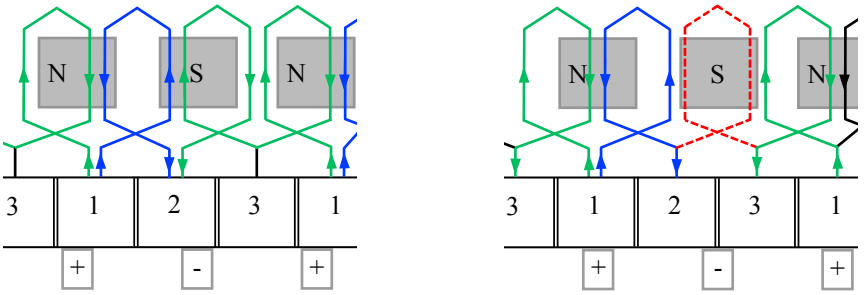

Fig. 2. (left) Winding diagram of 3-slot 2-pole brushed DC motor with marked current flow and (right) marked shorted winding during commutation.

For the current of the motor is valid:

$$U_s \cdot \mathrm{pwm}(t) = R_a i + L_a \frac{di}{dt} + u_{\mathrm{bemf}} \tag{2}$$

where pwm (t) is the binary function of the PWM controller (pulse wave), R_a is the resistance of the armature and L_a is its inductance. The current of the motor may be measured by measuring the voltage across current sensing bypass resistor. The signal needs to be amplified, filtered and digitally processed.

The motor is controlled by PWM (e.g. H-bridge). The supply voltage is therefore a pulse wave with frequency f_{PWM}. Commutator shortage occurs n-times per turn:

$$n = poles \cdot slots \tag{3}$$

The frequency of the current pulses is therefore:

$$f_{\mathrm{pulse}} = \frac{RPM}{60} n \tag{4}$$

Duration of the commutator shortage corresponds to the angular size of the commutator brush. The impedance of the armature is decreased during shortage by:

$$\Delta R = \frac{R_a}{slots} \tag{5}$$

The current of the motor contains three components:

- DC part – creating torque,
- fPWM – caused by controller,
- fpulse – caused by commutator, proportional to RPM.

The frequency of the PWM has to be much greater than the largest possible f_{pulse} in order to provide reliable detection. In our experiments we have used DC motor with 3 slots and 2 poles having maximal no-load speed 12 000 RPM at 12V supply voltage (K_V = 1000 RPM/V). The maximal possible pulse frequency is then $f_{pulse(max)}$ = 1.2 kHz. The selected PWM frequency is f_{PWM} = 62.5 kHz but it contains huge portion of higher harmonic frequencies.

Therefore, we have decided to use 4th order analog linear low-pass filter combined with 1st order high-pass filter in order to filter out the two remaining components (DC a PWM) of the current signal. Then, only valid pulses should remain in the signal.

3. Simulation and design

For the simulation and pre-verification of the designed sensor MATLAB was used. First, we simulate supply voltage with PWM and the changing impedance of the armature by two pulse waves. Then we compute the ideal current across the armature according to (2) neglecting the inductance of the armature:

$$i_{\text{ideal}}(t) = \frac{U_s \cdot \text{pulse}\left(2\pi f_{\text{PWM}} t, \delta\right) - K_u \omega}{(R_a - \Delta R) + \Delta R \cdot \text{pulse}(n\omega t, \sigma)} \tag{6}$$

where δ is a duty rate of the PWM control and σ is a duty rate of the commutator shorting effect. The function *pulse* is periodic, and the first period is defined as follows:

$$pulse(x,d) = \begin{cases} 1 & x \in \left[0, 2\pi d\right) + 2\pi k, \\ 0 & x \in \left[2\pi d, 2\pi\right) + 2\pi k. \end{cases} \tag{7}$$

The current smoothing effect caused by the inductance of the armature can be expressed by transfer function:

$$F_L(s) = \frac{1}{\frac{L_a s}{R_a} + 1} = \frac{1}{T_a s + 1} \tag{8}$$

where L_a is the inductance of the armature. The armature cannot feed current to the supply, therefore its current cannot be negative. Then we obtain the current of the motor:

$$i(t) = \max\left(L^{-1}\left\{F_L(s) \cdot I_{\text{ideal}}(s)\right\}, 0\right) \tag{9}$$

where $I_{\text{ideal}}(s)$ denotes Laplace *s*-domain function of the ideal armature current $i_{\text{ideal}}(t)$.
The block diagram of the sensor is in Fig. 3:

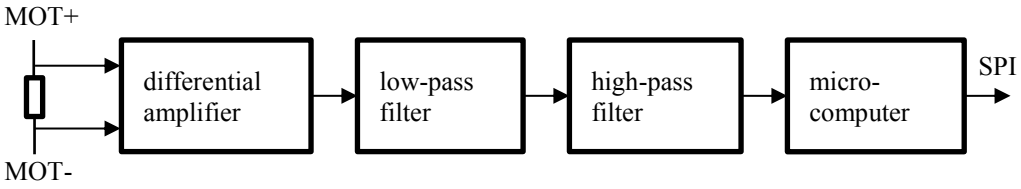

Fig. 3. Bock scheme of the sensor.

The transfer function of the input analog filter is:

$$F_f(s) = G_{IN} \cdot F_{LP}(s) \cdot F_{HP}(s) \cdot G_{OUT} = G_{IN} \cdot \frac{1}{\left(T_{LP} s + 1\right)^4} \cdot \frac{T_{HP} s}{\left(T_{HP} s + 1\right)} \cdot G_{OUT} \tag{10}$$

where G_{IN} is the gain of the input differential amplifier including measuring resistor, $F_{LP}(s)$ is the transfer function of the low-pass filter, $F_{HP}(s)$ is the transfer function of the high-pass filter and G_{OUT} is the gain of the output amplifier.

The cut-off frequency of the low-pass stage was set to f_{LP} = 5 kHz and the cut-off frequency of the high-pass filter is f_{HP} = 0.4Hz in order to allow full working range of the DC motor. All analog filters are active filters utilizing operational amplifiers (see Fig. 4.). Taking the output of the 2nd low-pass stage we also obtain DC current level. Used microcontroller has 5V supply voltage, therefore all signals need to be fitted into the range 0 ÷ 5V, therefore the centrum of the supply is artificial, generated by resistor divisor.

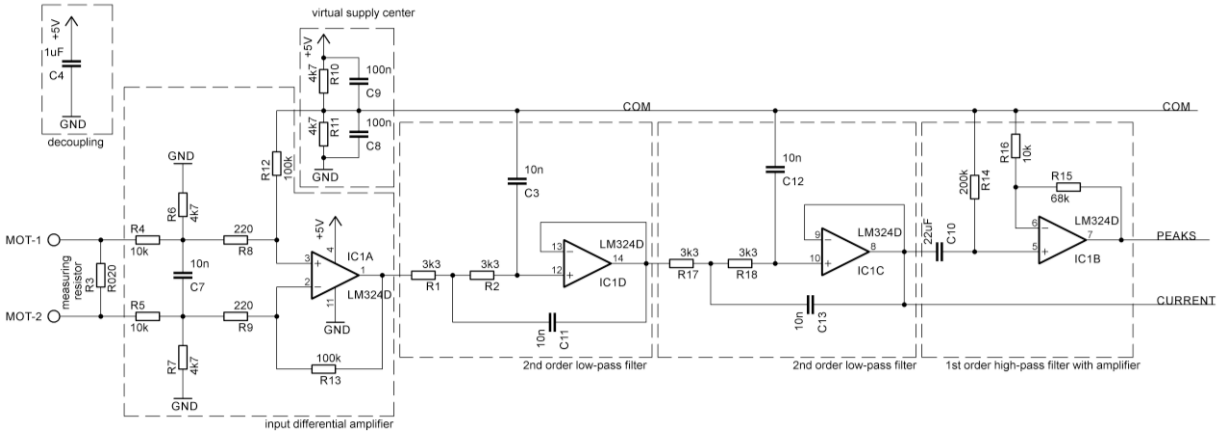

Fig. 4. Electrical scheme of the analog input filter.

True cut-off frequencies are:

$$f_{LP} = \frac{1}{2\pi T_{LP}} = \frac{1}{2\pi R_1 C_3} \approx 4.82 \text{ kHz} \quad , \qquad f_{HP} = \frac{1}{2\pi T_{HP}} = \frac{1}{2\pi R_{14} C_{10}} \approx 0.036 \text{ Hz} \, . \tag{11}$$

In order to allow full range of the motor's supply voltage (U_s = 12V), output of the current sensing resistor has to be scaled down to the logical level range. Gains of the input and output stage are:

$$G_{IN} = \frac{R_7}{R_5 + R_7} \cdot \frac{R_{13}}{R_9} \approx 145 \, , \qquad G_{OUT} = 1 + \frac{R_{15}}{R_{16}} \approx 7.8 \, . \tag{12}$$

Frequency characteristics of the designed filter is in Fig. 5.

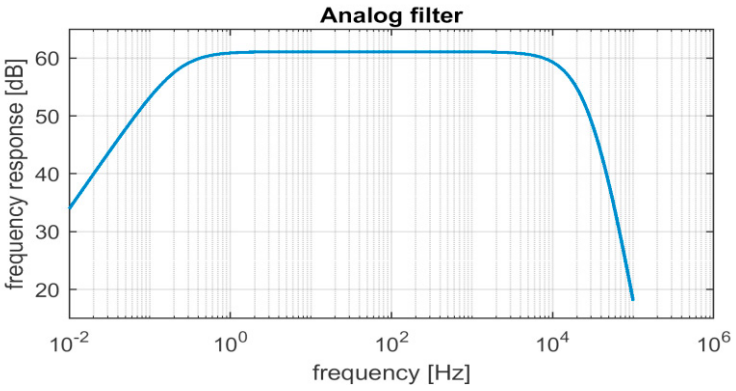

Fig. 5. Frequency response of the input filter.

Using above mentioned formulas we have computed theoretical current of the motor and the result output voltage (see Fig. 6.). The parameters of the motor were $R_a = 2\ \Omega$, $L_a = 20\mu H$, $\sigma = 83\%$, $\delta = 20\%$, poles = 2, slots = 3, $K_V = 1000$ RPM/V, $R_{measue} = 0.020\Omega$, speed of the motor was 1800 RPM.

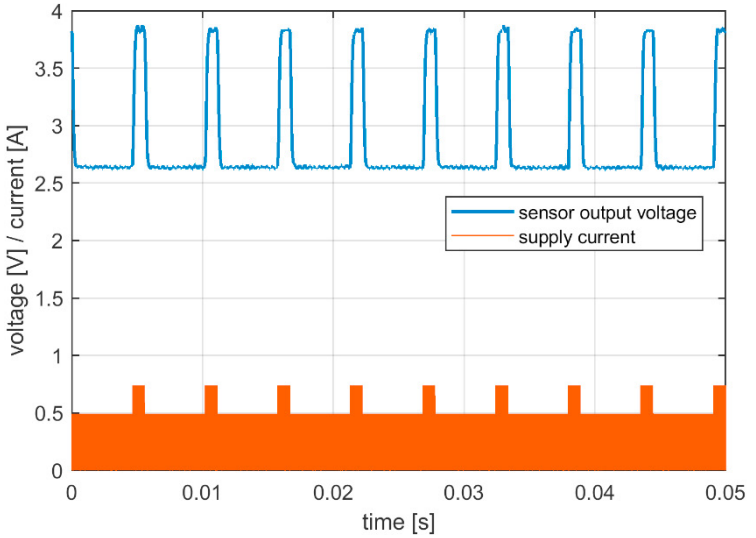

Fig. 6. Simulated current of the motor and the analog stage output voltage.

4. Digital processing

The output of the analog filtering stage has to be processed by the microcontroller. The input A/D converter is programmed to subtract the voltage of the artificial supply center COM from the voltage of the signal PEAKS (see Fig. 4.). First, we apply digital Chebychev low-pass filter to the digital signal sampled at 51.6kHz:

$$F_d(z) = \frac{3}{8} \cdot \frac{1 + 3z^{-1} + 3z^{-2} + z^{-3}}{1 + 2z^{-2}} \tag{13}$$

which characteristics is in Fig. 7. Its cut-off frequency is approx. 14kHz.

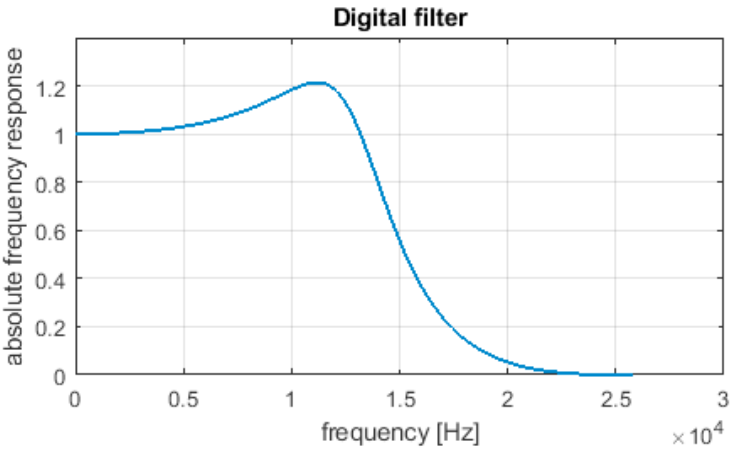

Fig. 7. Digital filter frequency characteristics.

The angular position of the motor is then computed by counting the peaks in the digitally-filtered signal.

5. Experiment

In the experiment we have used LM324D 4-channel operational amplifier for analog filtering and AtTiny44 microcontroller for digital processing. The output (count of pulses) is provided via SPI interface. The prototype of the sensor board is in Fig. 8. The parameters of the motor were same as the parameters used in simulation. Measured output of the analog filters is in Fig. 9. The true speed of the motor was 2039.5 RPM, measured frequency of the pulses is f_{pulses} = 203.97 Hz which corresponds to the speed 2039.7 RPM (= 60 * f_{pulses} / n).

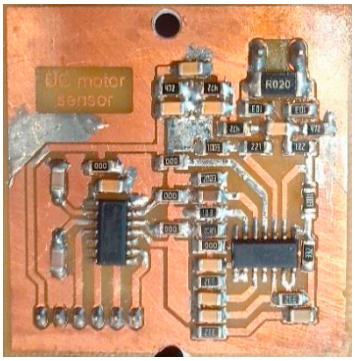

Fig. 8. Sensor board prototype.

As can be seen, the output of the analog filter is noisy, but it clearly contains pulses. The speed of the motor has been estimated correctly. The digital processing algorithm mentioned above filters out noisy spikes. The output of the analog filter is therefore sufficient and additional analog filtering stages are not required for proper function of the sensor.

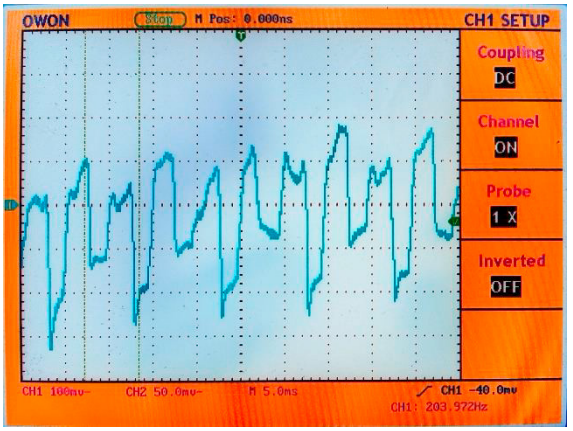

Fig. 9. Measured output of the analog filters.

6. Conclusion

Measuring the position and speed of a motor is widely required in both robotics and automotive industry. The proposed sensor is capable to detect position of a DC motor in wide interval of RPM. It does not require any mechanical components to be installed onto the shaft of the motor, therefore it is especially suitable for usage in applications where the dimensions of the motor are limited or the existing construction does not allow to add another type (mechanical,

magnetic, optic) of encoder. The proposed filtering and signal processing techniques were successfully verified using hardware prototype. The solution can be scaled by different choice of the current measurement resistor.

Acknowledgements

This work was supported by Slovak Research and Development Agency under the project no APVV-16-0006: 'Automated robotic assembly cell as an instrument of concept Industry 4.0'.

References

Chotai, J., Narwekar, K., 2017. Modelling and position control of brushed DC motor, in "International Conference on Advances in Computing" in "Communication and Control (ICAC3)", Mumbai, pp. 1-5. doi: 10.1109/ICAC3.2017.8318792

Afjei, E., Nadian Ghomsheh A., Karami, A., 2007. Sensorless speed/position control of brushed DC motor, in "International Aegean Conference on Electrical Machines and Power Electronics", Bodrum, pp. 730-732., doi: 10.1109/ACEMP.2007.4510598

Ramli, R. M., Mikami, N., Takahashi, H., 2010. Adaptive filters for rotational speed estimation of a sensorless DC motor with brushes, in "10th International Conference on Information Science", in "Signal Processing and their Applications (ISSPA 2010)", Kuala Lumpur, 2010, pp. 562-565, doi: 10.1109/ISSPA.2010.5605587

Kumar, T. S., Banavar, R. N., 2017, Observer based control of a brushed DC motor at very low speeds over controller area network, in "An application in astronomical telescopes", in "11th Asian Control Conference (ASCC)",pp. 1449-1453.doi: 10.1109/ASCC.2017.8287386

Kamdar, S., Brahmbhatt, H., Patel, T., Thakker, M., 2015. Sensorless speed control of high speed brushed DC motor by model identification and validation, in "5th Nirma University International Conference on Engineering (NUiCONE)", Ahmedabad, 2015, pp. 1-6., doi: 10.1109/NUICONE.2015.7449594

Rapos, D., Mechefske C., Timusk, M., 2016, Dynamic sensor calibration: A comparative study of a Hall effect sensor and an incremental encoder for measuring shaft rotational position, in "IEEE International Conference on Prognostics and Health Management (ICPHM)", Ottawa, ON, 2016, pp. 1-5. doi: 10.1109/ICPHM.2016.7542858

Vázquez, E., Sottile, J., Gomez-Gil, J., 2016, A Novel Method for Sensorless Speed Detection of Brushed DC Motors. Applied Sciences. vol. 7. issue 14. doi: 10.3390/app7010014.